remote sensing

Article

Evolution of Small and Micro Wetlands and Their Driving Factors in the Yangtze River Delta—A Case Study of Wuxi Area

Jiamin Zhang [1], Lei Chu [1], Zengxin Zhang [1,*], Bin Zhu [1], Xiaoyan Liu [1] and Qiang Yang [2]

[1] Joint Innovation Center for Modern Forestry Studies, College of Forestry, Nanjing Forestry University, Nanjing 210037, China
[2] College of Civil Engineering, Nanjing Forestry University, Nanjing 210037, China
* Correspondence: zzhang@hhu.edu.cn

Abstract: Understanding the long-term dynamics and driving factors behind small and micro wetlands is critical for their management and future sustainability. This study explored the impacts of natural and anthropogenic factors on the spatiotemporal evolution of these areas in Wuxi area using the support vector machine (SVM) classification method and the geographic detector model based on Landsat satellite image data from 1985 to 2020. The results revealed that: (1) Natural wetlands were prominent in Wuxi area, with an average proportion of 70%, and although they exhibited a downward trend over the last ten years, the scale of natural small and micro wetlands increased 1.5-fold—from 4349.59 hm^2 in 1985 to 10,841.59 hm^2 in 2020. (2) The small and micro wetlands in Wuxi area had obvious seasonal variations, with most being 0.1–1 hm^2 and 1–3 hm^2, respectively. From the perspective of spatial distribution, they were primarily distributed in Yixing district, which accounts for 34% of Wuxi area. (3) The distribution of small and micro wetlands was systematically affected by natural and human activities. The main factors that affected the distribution of small and micro wetlands were the average annual temperature and GDP, with the interactions between all factors being nonlinear and bi-linear. The influences of natural factors on small and micro wetlands were weakened, with human activities steadily emerging as the dominant factor that affected their distribution. The results of this study can provide supportive data and a scientific basis for the ecological restoration and protection of wetlands.

Keywords: Wuxi area; natural wetland; small and micro wetlands; driving factors; geographical detector

Citation: Zhang, J.; Chu, L.; Zhang, Z.; Zhu, B.; Liu, X.; Yang, Q. Evolution of Small and Micro Wetlands and Their Driving Factors in the Yangtze River Delta—A Case Study of Wuxi Area. *Remote Sens.* **2023**, *15*, 1152. https://doi.org/10.3390/rs15041152

Academic Editor: Dehua Mao

Received: 30 December 2022
Revised: 13 February 2023
Accepted: 15 February 2023
Published: 20 February 2023

1. Introduction

Wetlands are among the most productive and sensitive ecosystems in the world [1]; they provide indirect, albeit essential, ecosystem services such as water conservation [2], water purification, carbon sequestration, and biodiversity conservation. The spatial distribution of wetlands is a heterogeneous network comprising many small and micro wetlands, as well as a few large wetlands. Small and micro wetlands are important for the support of biodiversity [3], as they can serve as transit sites for species migration, provide critical habitats for certain insects, waterbirds, etc., and support endangered species and the richness of rare species more effectively than large wetlands [4]. Small and micro wetlands are highly sensitive to hydrological and climatic conditions, and the loss of small and micro wetlands significantly weakens the structures and functional characteristics of ecological networks [5]. Small and micro wetlands also provide critical watershed functions; thus, their disappearance will seriously impact the potential for nutrient treatment at the landscape scale. Therefore, they must be more seriously considered in wetland conservation and restoration efforts [6]. Recently, researchers have mainly focused on the functions of independent small and micro wetlands at small regional scales, particularly small and micro wetlands in ponds and lakes [7,8]. However, there is a lack of specific discourse on the overall changes and driving factors behind small and micro wetlands at the regional scale [9–11].

The current research method for small and micro wetlands is mainly a field survey; however, unmanned aerial vehicle (UAV) detection and remote sensing interpretation are also utilized [12–14]. Although field surveys provide accurate data, they are time-consuming and slow to update [7]. On the other hand, UAVs offer continuous dynamic detection, and they come at a higher cost [14]. Remote sensing technology, with its strong timeliness, wide coverage, large amount of information, and short update period, is an indispensable technical tool for wetland surveys [15–17]. Currently, the extraction of wetland information is mainly based on Landsat series, Sentinel series, and other high-resolution satellite images [18–20]. The main methods used to extract information about wetland water bodies are the threshold value method, the water body index method, and algorithmic model extraction [21,22]. The threshold method is simple to calculate, but the threshold value is often difficult to determine, resulting in unstable classification results [23]. Water body index methods, such as the commonly used NDWI (normalized difference water index), MNDWI (modified normalized difference water index), and NDVI (normalized difference vegetation index) indicators, are more widely used and provide better results [24,25]. The NDWI index is helpful for distinguishing open water conditions, the MNDWI index facilitates the classification of areas characterized by shallow water, mud, and vegetation mosaics, and the NDVI index can easily distinguish bare soil from vegetated soil [26]. The algorithmic model extraction is not universally applicable, although it is accurate [27]. In terms of classification, the most recent applications include traditional supervised and unsupervised classification, as well as machine learning algorithms such as random forest (RF) and support vector machines (SVM) [28,29]. Traditional manual visual classification has high accuracy but is time-consuming and prone to errors [30]. The RF classification can determine the optimal parameter combination based on the number of regression trees (t) and the number of variables used by each node in the tree (m), and it can carry out training samples, but it is easy to overfit [31]. The SVM algorithm has the advantages of small sample training and support for high-dimensional feature spaces, along with high accuracy and wide applicability [32], which have been verified in the studies of Balogun et al. [33], Ghosh et al. [34], and Zhang et al. [35]. Therefore, based on Landsat series images with a long time series, this paper intends to use the water index method for feature extraction and SVM classification for interpretation to obtain the information of small and micro wetlands in the study area.

A number of studies have found that wetlands in various regions are facing threats from both natural and anthropogenic factors, such as climate change and alterations in land use and land cover [36]. These factors exert linear as well as non-linear impacts on wetland changes, making it crucial to understand the drivers of these changes [37]. Previous studies have investigated the reasons for the decline in small and micro wetlands and identified several potential factors, such as socio-economic factors such as urbanization-induced shifts in land use, changes in population density, and road networks and natural factors such as climate and topography [38–40]. The methods employed to study the drivers of changes in small and micro wetlands include logistic regression, correlation analysis, and cluster analysis [41–43]. The geodetector model is a statistical approach based on spatial ANOVA for the detection of spatial heterogeneity and the exploration of its driving mechanisms [44]. It overcomes the limitations of traditional statistical methods and can accurately identify the contribution of individual factors and their interactions, as well as test for significant differences between groups [45]. The geodetector model has been successfully applied to the study of spatial differentiation and influencing factors in the contexts of urbanization expansion [46], land use change [47], vegetation cover change [48], landslides [49], wetland change [50], etc. Therefore, the geodetector model can be utilized to study the causes of small and micro wetland changes.

The Yangtze River Delta region, the second-largest delta in the world, holding more than one-fifth of China's wetland resources. However, while most of the large wetlands in the watershed have been explored, little research has been conducted on small and micro wetlands, and there is a scarcity of basic data. This study seeks to address this gap by using

Landsat imagery from 1985 to 2020 to extract wetlands in Wuxi through SVM classification and explores the influencing factors on the evolution of small and micro wetlands in Wuxi area by combining this with the geodetector model. The study aims to: (1) analyze the spatiotemporal distribution and dynamic changes of small and micro wetlands in Wuxi over the past 35 years; (2) explore the relationship between small/micro wetlands and wetland change in Wuxi area; and (3) quantify the contribution of climate change and human activities to the changes in micro and small wetlands. This study is helpful in understanding the changes of small and micro wetlands under the influence of climate change and strong human activities, and it also provides ideas for the research of small and micro wetlands in other areas.

2. Materials and Methods

2.1. Study Area

Earlier studies have investigated wetlands on a large scale; however, they have rarely been investigated at small and medium scales. To illustrate the evolution of small and micro wetlands in the Taihu Lake Basin, this investigation selected Wuxi area as the study region, including the urban and rural areas under its jurisdiction: Jiangyin district, Huishan district, Xishan district, Liangxi district, Jingkai district, Xinwu district, Binhu district, and Yixing district, which is situated between 31°07′N–32°02′N and 119°33′E–120°38′E. Wuxi is an important prefecture-level metropolis in the Taihu Lake Basin of the Yangtze River Delta corridor, with a total area of 4628 km^2. It is home to a humid subtropical monsoon climate, with high temperatures and rainfall in the summer and mild, dry winters. The annual average temperature and precipitation are 16.2 °C and 1121.7 mm, respectively. The city is dominated by a plain that faces the Yangtze River in the north, is crisscrossed by rivers and lakes, and has numerous and widely distributed wetlands. The total wetland area accounts for ~22.5% of the national land area. In 2020, the conservation rate of natural wetlands reached 62% (Figure 1).

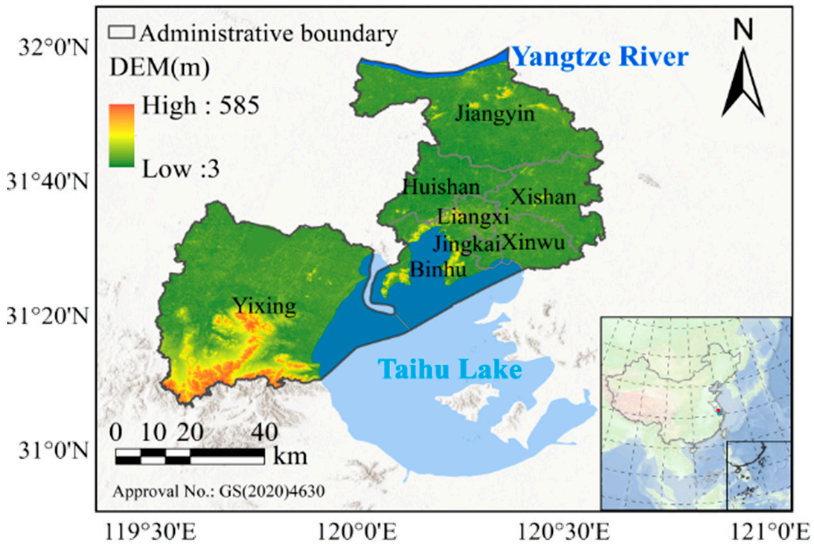

Figure 1. Location of the Wuxi area.

2.2. Data Sources

Remote sensing datasets were obtained from the United States Geological Survey (USGS, https://www.usgs.gov/, accessed on 30 September 2021). Landsat images were selected from Landsat 4/5 TM and Landsat 8 OLI, with a spatial resolution of 30 m × 30 m and a row number of 119/38. The image follows the selection of plant growing season months and cloud cover <10% as far as possible. Under the influences of cloud cover interference and image quality, 11 scene image data were selected (Table 1).

Table 1. Description of data used in the present study.

Data Type	Data	Year	Date of Acquisition	Spatial Resolution (m)	Sources
Remote sensing	Landsat 4/5 TM	1980	01/11	30 × 30	USGS: https://www.usgs.gov/ (accessed on 30 September 2021)
		1990	10/08	30 × 30	
		2000	04/26, 06/13, 09/17	30 × 30	
		2010	05/24, 10/31, 12/18	30 × 30	
	Landsat 8 OLI	2020	03/16, 05/19, 09/08	30 × 30	
Natural factors	Temperature	2000, 2010, 2020		1000 × 1000	The National Meteorological Information Center (http://data.cma.cn/, accessed on 28 July 2022)
	Precipitation			1000 × 1000	
	DEM, Slope	2020		30 × 30	Geospatial Data Cloud: http://www.gscloud.cn/ (accessed on 28 July 2022)
Anthropogenic factors	Population	2000–2020		1000 × 1000	WorldPop: https://www.worldpop.org (accessed on 28 July 2022)
	Gross Domestic Product (GDP)	2000–2020		1000 × 1000	Resources and Environmental Sciences: http://www.resdc.cn and Wuxi Statistical Yearbook (accessed on 28 July 2022)
	Roads	2000–2020			Openstreetmap: https://www.openstreetmap.org (accessed on 28 July 2022)
	Land use/land cover	1985		30 × 30	Resources and Environmental Science Data Center of the Chinese Academy of Sciences: http://www.resdc.cn (accessed on 28 July 2022)
		1990			
		2000			
		2010			
		2020			

The temperature and precipitation data (2000–2020) were collected from the National Meteorological Information Center (http://data.cma.cn/, accessed on 28 July 2022). ANUSPLIN 4.2 software was used to interpolate the raster meteorological data, after which the ArcGIS raster computing tool was used to calculate the average annual temperature and precipitation. The Global Digital Elevation Model (GDEM), with a resolution of 30 m, was downloaded from the Geospatial Data Cloud (http://www.gscloud.cn/, accessed on 28 July 2022), and the DEM slope was extracted using ArcGIS software.

Population density data (2000–2020) were obtained from the WorldPop dataset (https://www.worldpop.org (accessed on 28 July 2022)), with a resolution of 1 km. The GDP data (2000–2020) were obtained from the Resources and Environmental Sciences (http://www.resdc.cn, accessed on 28 July 2022) of the Chinese Academy of Sciences and Wuxi Statistical Yearbook, with a resolution of 1 km after spatial interpolation. The vector data for major roads (e.g., national and provincial roads) and railways were from Openstreetmap (https://www.openstreetmap.org, accessed on 28 July 2022), with a resolution of 1 km, and the distances from the main roads were calculated using the Euclidean distance method. The land use and land cover data (1980–2020) were obtained from the Resources and Environmental Science Data Center of the Chinese Academy of Sciences (http://www.resdc.cn, accessed on 28 July 2022). The spatial resolution was 30 m, and the land use types were divided into six categories (cultivated land, woodland, grassland, water, construction land, and unused land). Basic geographic data (study boundary) were acquired from the National Geographic Information Center of China (NGCC, http://www.NGCC.cn, accessed on 28 July 2022).

2.3. Methodology

The method flow chart of this study is depicted in Figure 2. The method framework consists of three major parts. First, enhanced images were obtained based on NDVI and MNDWI, interpretation markers were established, SVM was used to extract wetland information in the region, and the dynamic change characteristics of small and micro wetlands were obtained from remote sensing images. Second, the transfer matrix of land use types including wetlands was obtained by reclassifying the data of land use types. The CA-Markov model was applied to predict the future wetland change trend. Finally, the driving factors were analyzed using the geographic detector, and the influences of natural factors and human activities on the changes in small and micro wetlands were discussed.

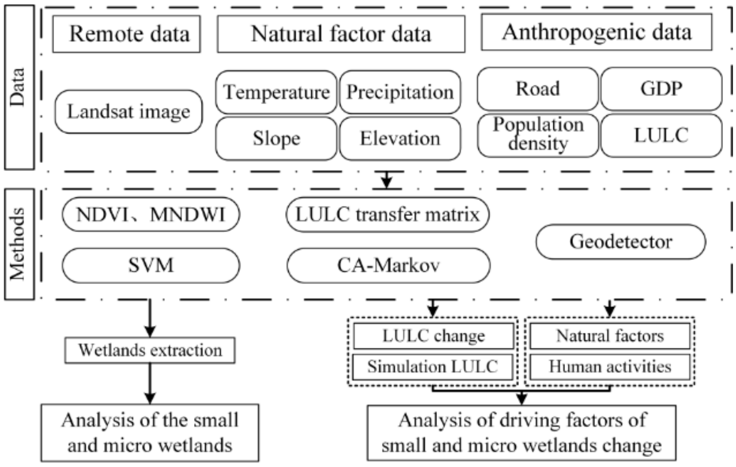

Figure 2. Methodology framework of this study.

2.3.1. Wetland Dynamic Analysis

Wetlands are threatened on a global scale due to anthropogenic activities and climate change, manifested as reduced wetland areas and changes in vegetation or land cover. Understanding these changes can assist with the protection of wetland ecosystems. In the literature, there is no clearly defined spatial range and water depth for small and micro wetlands, and the area threshold for distinguishing them is broad and diverse. Based on the universal definition of wetland in the world and considering the characteristics of wetlands, for this study, water bodies with an annual or seasonal presence of water, an average depth < 4 m, and areas of <8 hm^2, including lakes, swamps, reservoirs, and rivers with widths of <10 m and lengths of <5000 m, were defined as small and micro wetlands.

In this study, ENVI 5.3 was employed to conduct a series of image preprocessing tasks (e.g., mosaic cutting, radiometric calibration, atmospheric correction, etc.) on the acquired remote sensing images, after which the modified normalized water index (MNDWI) was used for water extraction. The normalized difference vegetation index (NDVI) was used for vegetation extraction, and the corresponding enhanced images were obtained. The interpretation signs were established based on the salient features of the enhanced images. The support vector machine classification (SVM) was utilized to extract the wetland data for the region. Using the Kappa coefficient and the overall accuracy test, the data was transferred to ArcGIS 10.5 for manual visual interpretation. The small and micro wetlands were classified to acquire the spatial and temporal characteristics of their changes in Wuxi area. The calculation formulae of the improved normalized water and vegetation indices are as follows:

$$W_{MNDWI} = \frac{B_{Green} - B_{MIR}}{B_{Green} + B_{MIR}} \tag{1}$$

where B_{Green} represents the reflectance of the green light band (band 2 in TM data and band 3 in OLI data); B_{MIR} represents the mid-infrared band (band 5 in TM data and band 6 in OLI data) reflectance [51].

$$W_{NDVI} = \frac{B_{NIR} - B_{RED}}{B_{NIR} + B_{RED}} \quad (2)$$

where B_{NIR} represents the reflectance of the near-infrared band (band 4 in TM data and band 5 in OLI data); B_{RED} refers to the red light band (band 3 in TM data and band 4 in OLI data) reflectance [52].

To effectively understand the processes involved in wetland changes (based on land use data from 1980 to 2020), the land use transformation matrix was used to analyze the spatiotemporal changes in land use. Changes in Wuxi area wetlands were quantitatively analyzed and supplemented, and the CA-Markov model was used to predict the land use status of Wuxi area in 2030. The land use transfer matrix is a method used to describe the directions and levels of changes in land use type transfers [53]:

$$L_{(t+1)} = P_{ij} \times L_{(t)} \quad (3)$$

$$P = \begin{bmatrix} P_{11} & P_{12} & \ldots P_{1m} \\ P_{21} & P_{22} & \ldots P_{2m} \\ P_{m1} & P_{m2} & \ldots P_{mm} \end{bmatrix} \quad (4)$$

where $L_{(t+1)}$ and $L_{(t)}$ are the land use/land cover conditions at (t + 1) and (t), respectively, and P_{ij} is the transition probability matrix of a certain state. Furthermore, $0 \leq P_{ij} < 1$ and $\sum_{j=1}^{m} P_{ij} = 1$ ($i, j = 1, 2, \ldots m$) comprise the migration probability matrix. Specific procedures can be found in the literature [54,55].

2.3.2. Analysis of Driving Factors behind Wetland Changes

1. Factors selection

To detect the drivers behind the changes in the small and micro wetlands of Wuxi area, four individual factors were selected for this study (distance from main roads ($X1$), average GDP ($X2$), population density ($X3$), and land use type ($X4$)). Two natural factors (annual precipitation ($X5$) and annual average temperature ($X6$)) and two topographic factors (slope ($X7$) and elevation ($X8$)) were used to detect changes in the Wuxi wetlands (Table 2). The wetland change area was taken as the dependent variable, and the eight driving factors were taken as independent variables (Table 3). Based on Create Fishnet in ArcGIS 10.5, 1 km × 1 km, 2 km × 2 km, 3 km × 3 km, 4 km × 4 km, and 5 km × 5 km grids were created. A total of 4989, 1318, 612, 360, and 236 sample points were generated, respectively, and a 2 km × 2 km grid was determined following the optimal scale selection [56]. The input variables of the Geodetector model can only be discrete variables. Thus, the selected factors were discretely transformed and reclassified into six categories based on the natural break point method (Figure 3). Subsequently, the Extract Values to Point function in ArcGIS was utilized to extract the data of all variables according to the locations of sample points. The single-factor contributions of small and micro wetlands, as well as the relationships between small and micro wetlands and driving factors, were quantified.

Table 2. Influencing factors of small and micro wetlands change.

Categories	Factors	Code	Unit
Anthropogenic activity	Distance to main roads	X1	km
	GDP	X2	10^4 yuan/km^2
	Population density	X3	person/km^2
	Land-use type	X4	categorical
Climate	Average annual precipitation	X5	mm
	Average annual temperature	X6	°C
Topography	Slope	X7	degree
	Elevation	X8	m

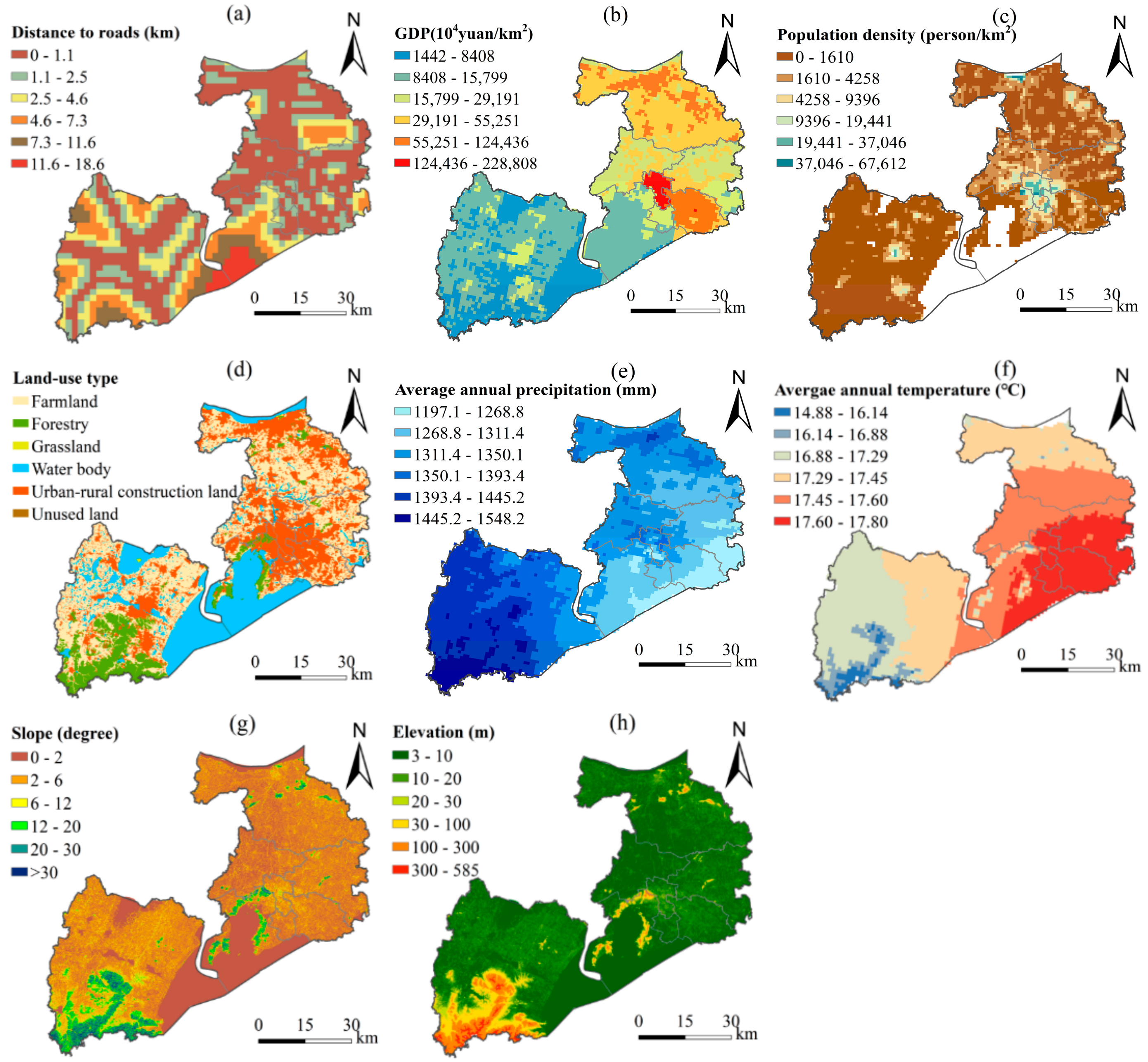

Figure 3. Spatial distribution characteristics of natural and anthropogenic factors in Wuxi area, 2020: factorial distribution of distances from major roads (**a**), GDP (**b**), population density (**c**), land use type (**d**), average annual precipitation (**e**), average annual temperature (**f**), slope (**g**) and elevation (**h**).

Table 3. Factors grading standards.

Categories \Factors	Distance to Main Roads	GDP	Population Density	Land-Use Type	Average Annual Precipitation	Average Annual Temperature	Slope	Elevation
1	0–1.1	1442–8408	0–1610	Farmland	1197.1–1268.8	14.88–16.14	0–2	3–10
2	1.1–2.5	8408–15,799	1610–4258	Forestry	1268.8–1311.4	16.14–16.88	2–6	10–20
3	2.5–4.6	15,799–29,191	4258–9396	Grassland	1311.4–1350.1	16.88–17.29	6–12	20–30
4	4.6–7.3	29,191–55,251	9396–19,441	Water body	1350.1–1393.4	17.29–17.45	12–20	30–100
5	7.3–11.6	55,251–124,436	19,441–37,046	Urban–rural construction land	1393.4–1445.2	17.45–17.60	20–30	100–300
6	11.6–18.6	124,436–228,808	37,046–67,612	Unused land	1445.2–1548.2	17.60–17.80	>30	300–585

2. Geodetector Model

Both natural and anthropogenic factors can have significant impacts on wetlands. Geographical detectors are used extensively to analyze the mechanisms of various influencing factors due to their unique advantages. General geographical detectors include four components: the core, which is a factor detector that quantifies the relative importance of different geographical variables, working in conjunction with interaction, risk, and ecological detectors [57]. For this paper, the driving factors of changes in small and micro wetlands were primarily analyzed through factor and interaction detectors.

The general form was as follows:

(1) Factor detector

This module was used to detect the spatial heterogeneity of variables and the extent to which factors explained the spatial heterogeneity of variables [50]. The q statistic value was employed to quantitatively detect the explanatory degree of driving factors for the spatial differentiation of small and micro wetlands.

$$q = 1 - \frac{SSW}{SST} \tag{5}$$

$$SSW = \sum_{h=1}^{L} N_{h^{\sigma_h^2}}, \; SST = N_{\sigma^2} \tag{6}$$

where q represents the explanatory power of driving factors for small and micro wetlands in the area; SSW is the sum of variance of the factors within all layers; and SST is the total variance of the whole region. h is the hierarchy of the class number of driver X, $h = 1, \ldots$; L is the number of layers of the dependent variable or independent variable; N_h and N are the number of units in layer h and that in the entire region, respectively; σ_h^2 and σ^2 are the variances of the attribute values of the dependent variable at layer h and the whole region, respectively [44]. The statistical value of q is between [0,1], which increases with the intensity of stratified heterogeneity [58]. The larger the q value, the greater the explanatory power of driving factor X for small and micro wetlands. The specific calculation steps and an explanation of the equations can be found in the literature [59,60].

(2) Interaction detector

This module can identify the interactions between the two drivers for the wetland. Initially, the q values of the two driving factors of wetlands ($q(X1)$ and $q(X2)$) were calculated, respectively, and the two layers of variables $X1$ and $X2$ were superimposed to obtain a new layer: $X1 \cap X2$ (interaction was denoted by $\cap$ in this study), after which the q value of the interactive effect ($q(X1 \cap X2)$) was calculated and compared with $q(X1)$ and $q(X2)$ to determine the interaction modes between the two driving factors (Table 4) [61–63].

Table 4. Interaction detection types.

Interaction Relationship	Interaction
$q(X1 \cap X2) > q(X1) + q(X2)$	Enhanced, nonlinear
$q(X1 \cap X2) = q(X1) + q(X2)$	Independent
$q(X1 \cap X2) > \mathrm{Max}(q(X1), q(X2))$	Enhanced, double factors
$\mathrm{Min}(q(X1), q(X2)) < q(X1 \cap X2) < \mathrm{Max}(q(X1), q(X2))$	Weakened, single-factor nonlinear
$q(X1 \cap X2) < \mathrm{Min}(q(X1), q(X2))$	Weakened, nonlinear

3. Results

3.1. Dynamic Changes in Natural Wetlands and Small-Micro Wetlands of Wuxi Area

In this study, the Support Vector Machine (SVM) was used for wetland extraction, and all the classification results passed the Kappa coefficient validation (all Kappa coefficients >0.9) and the overall accuracy validation (overall accuracy verification >95%) with a high classification accuracy. Further, combined with the paddy field data during the study period, the natural wetland stripping was realized based on the ArcGIS Erase tool.

According to the calculations, Wuxi area is dominated by natural wetlands, where the multi-year average retention of natural wetlands was stable at 79% during the study period. Therefore, this study is focused on the natural small and micro wetlands of Wuxi area. To further verify the accuracy of the natural small and micro wetlands, we randomly selected several sample areas in the study area to be compared with the third adjustment data of the National Land Survey published by Wuxi Municipal Government, using 2020 as an example. The error values were obtained (Table 5). It is not difficult to find that the error values were small.

Table 5. Accuracy verification of remote sensing image extraction data.

Serial Number	Geographical Coordinate	Image Extraction Area (hm^2)	Field Survey Area (hm^2)	Difference (hm^2)	Error (%)	Location
1	31°14′N, 119°46′E	4.76	4.83	−0.07	−1.45	Yixing district
2	31°15′N, 119°50′E	2.41	2.50	−0.09	−3.60	
3	31°33′N, 120°13′E	2.93	2.98	−0.05	−1.68	Binhu district
4	31°35′N, 120°6′E	4.71	4.88	−0.17	−3.48	Huishan district
5	31°46′N, 120°34′E	1.85	1.94	−0.09	−4.64	Jiangyin district
6	31°52′N, 120°4′E	2.23	2.33	−0.10	−4.29	

As shown in Figure 4, the natural wetland resources of Wuxi exhibited a fluctuating growth trend from 1985 to 2020 but have shown a degrading trend since 2010. From 1985 to 2010, the wetland area increased significantly—from 8.68×10^4 hm^2 in 1985 to 10.33×10^4 hm^2 in 2010—which translated to an increase of ~19%. Following 2010, the total natural wetlands area decreased by 10% to ~9.39×10^4 hm^2. In terms of quantity, the number of natural wetlands in Wuxi area reached 1.50×10^4 in 2020, which was nearly 2.7 times that in 1985 (0.55×10^4). In terms of administrative regions, Yixing district and Binhu District were the top areas for natural wetlands, at 44% and 38%, respectively, by 2020. The trends in changes in wetland areas in each district were basically consistent with those of the total natural wetland area changes in Wuxi area, where, after a continuous increase until 2010, there was a decline over the last decade. Among them, Liangxi District and Xinwu District lost more natural wetlands area compared with the value in 1985, decreasing by 59% and 23%, respectively. In contrast, the natural wetland areas in Yixing and Huishan Districts showed an increasing trend prior to 2000 but underwent a continued decrease subsequently.

In terms of area, the natural small and micro wetlands in Wuxi area were divided into four categories (0.1–1 hm^2, 1–3 hm^2, 3–5 hm^2, and 5–8 hm^2). Figure 5 reveals the spatial distribution and proportion of small and micro wetlands for each district. From the spatial distribution, the micro and small wetlands in Wuxi were mainly distributed in Yixing district, and the area of natural micro and small wetlands accounted for 34% of Wuxi area. It was observed that the small and micro wetland areas of each district in Wuxi were mainly 0.1–1 hm^2 and 1–3 hm^2, with an average proportion of 38% and 32%, respectively. The area and patch number of small and micro wetlands increased, particularly in Yixing and Jiangyin Cities. It is worth noting that although the scale of natural small and micro wetlands in each district increased, the spatial composition of natural small and micro wetlands in each district was significantly altered, where the proportion of 3–5 hm^2 and 5–8 hm^2 in each district decreased significantly after 2010, with an average proportion of only 13% and 12%, respectively. The spatial and temporal distributions of small and micro wetlands have also changed. The distribution of small and micro wetlands in the south of Jiangyin district was higher before 1990, while the distribution of small and micro wetlands along the Yangtze River in Jiangyin district increased significantly after 1990. Prior to 2000, many wetlands were distributed in the southern portion of Yixing district; however, by 2020, this trend was reversed. Many small and micro wetlands were distributed in the northern portion of Yixing, with Ge Lake as the central site.

The change trend of the total number and area of natural small and micro wetlands in Wuxi area has been consistent with that of the total area, which has increased over the last 35 years (Figure 6a). In terms of area, most natural small and micro wetlands in

Wuxi are 0.1–1 hm^2 and 1–3 hm^2. In 1985, the natural small and micro wetlands area was ~4349.59 hm^2, whereas in 2020, it was ~10,841.59 hm^2, which was ~1.5-fold higher. In terms of quantity, Wuxi is dominated by small and micro wetland patches (0.1–1 hm^2), which will diminish with increased patch areas. In 2020, the number of small and micro wetland patches at 0.1–1 hm^2 accounted for 81%, while the number of other types of small and micro wetland patches accounted for 14%, 3%, and 2%, respectively. In 1985, the number of natural small and micro wetland patches in Wuxi area was 5366, whereas in 2020, it was 14,690, an increase of nearly 1.7 times.

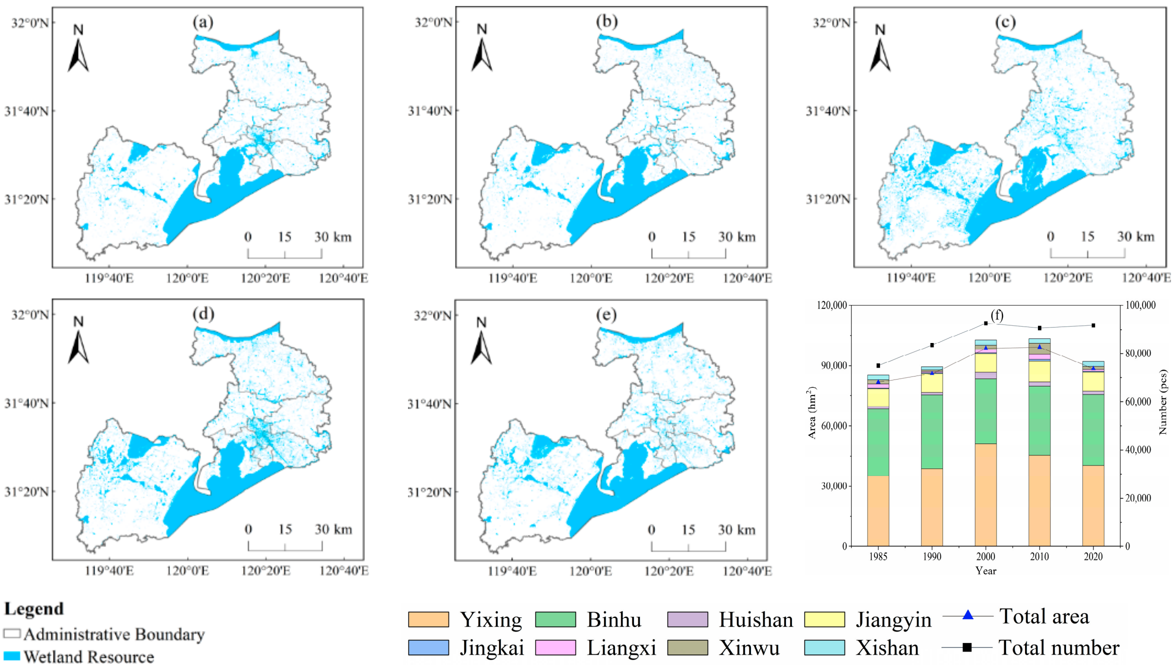

Figure 4. Changes in natural wetlands in Wuxi area from 1985 to 2020: 1985 (**a**), 1990 (**b**), 2000 (**c**), 2010 (**d**), 2020 (**e**), and district area overlay map (**f**).

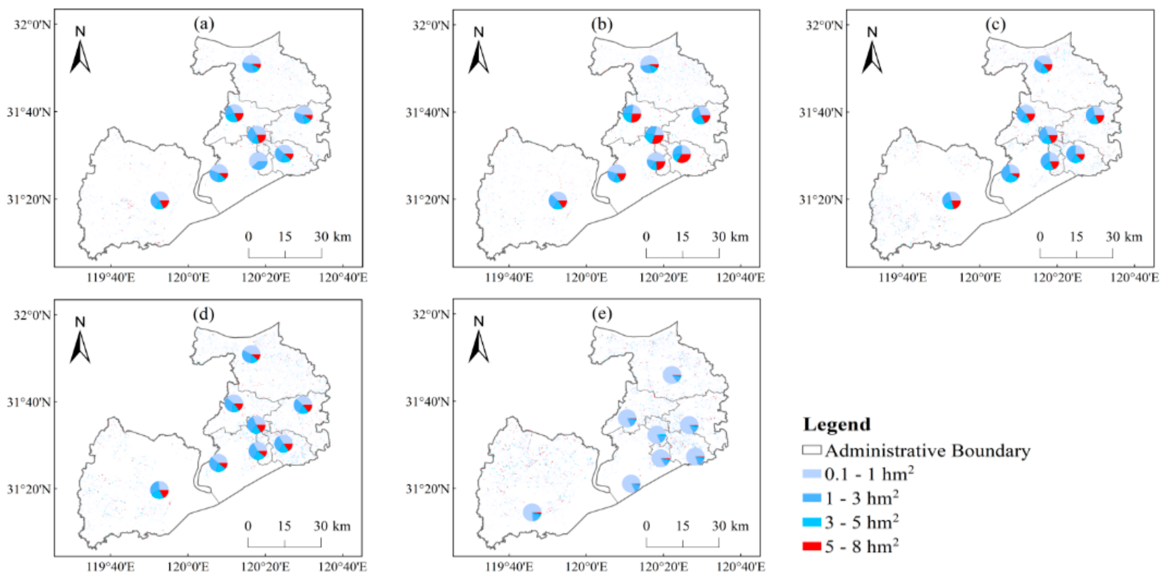

Figure 5. Changes in natural small and micro wetlands in Wuxi area from 1985 to 2020: 1985 (**a**), 1990 (**b**), 2000 (**c**), 2010 (**d**), 2020 (**e**). (The pie chart represents the area proportion of the four types of small and micro wetlands in each district).

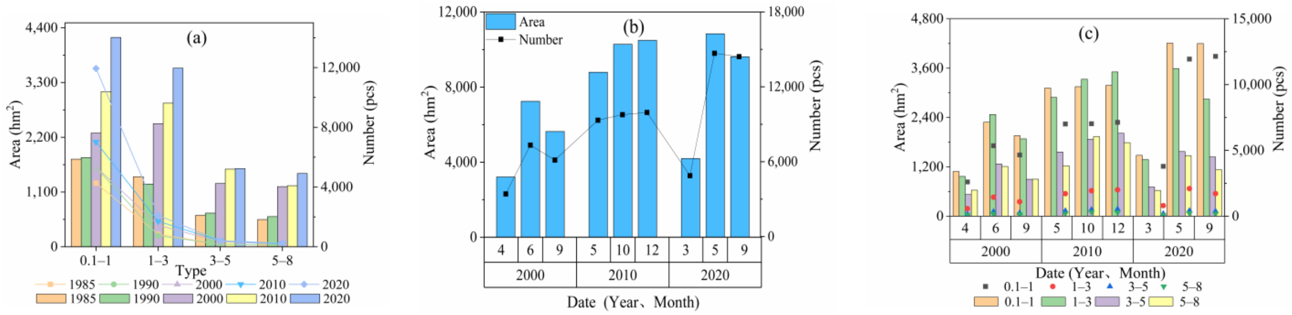

Figure 6. Interannual variations of natural small and micro wetlands in Wuxi from 1985 to 2020 (**a**), and overall (**b**) and within-group seasonal variations (**c**) from 2000 to 2020.

Seasonal changes in the natural small and micro wetlands of Wuxi from 2000 to 2020 were further analyzed (Figure 6b) and were found to be obvious, with more and expanded wetland areas during the summer and autumn and fewer wetland areas in the spring. In contrast to the year 2000, both the numbers and areas of small and micro wetlands increased significantly in Wuxi, increasing by 31% by the spring of 2020, by 50% in summer, and by 71% in autumn. The number of wetlands increased by 43% in the spring and nearly doubled in summer and autumn. This confirmed that the small and micro wetlands in Wuxi were extensively fragmented and that wetland resources were patched. Seasonal variations within groups were also analyzed for small wetlands (as shown in Figure 6c). The results showed that the trends of seasonal changes in small wetlands of all categories aligned with the overall trend. However, compared to 2000, the proportion of other categories of small wetlands in summer and autumn declined continuously, except for small and micro wetlands, with an area of 0.1–1 hm^2 as of 2020. Notably, the seasonal changes of small and micro wetlands with an area of 5–8 hm^2 have stabilized over the past 20 years, with only a 0.2% change in each season. The trends of seasonal changes in the number of small wetlands in each category followed the trends of changes in area. The smaller wetlands (0.1–1 hm^2) have become more prominent in terms of their proportion and more sensitive to seasonal fluctuations, indicating the increased vulnerability of smaller wetlands to seasonal disturbances.

3.2. Relationship between Wetlands and Land Use in Wuxi Area

Wetlands are an important type of land use and land cover. The extent of land use (LULC) changes in the study area (Figure 7) and the Sankey diagram that reflected them (Figure 8) revealed that the largest proportion of land use was arable land. The land use transfer matrix is a tool used to quantify the changes in land use types. It does this by analyzing the shift in land use from the start to the end of the study period. Inflow refers to the transformation of one land class into another, while outflow refers to the transformation of one land type into other land types. The inflow and outflow reflect the area and structure transformation of each land type, and we can understand the general change trend and structural change of regional land use types [64]. The overall attributes of land use changes in Wuxi area (1980–2020) encompassed urbanization, a rapid increase in urban and rural construction, and a sharp decrease in cultivated land. From 1980 to 2020, the various types of land use were significantly altered, with the greatest changes occurring in the inland portions of the study area via urban and rural construction. The urban and rural construction area in Wuxi more than tripled, climbing from 40,167.63 hm^2 in 1985 to 131,385.42 hm^2 in 2020, with the total land category proportions increasing from 6.23% to 19.54%, respectively. The inflow of urban and rural construction land (103,513.56 hm^2) comprised mainly arable land (88,265.78 hm^2), followed by natural wetlands, small and micro wetlands, and woodlands. There was also a small amount of grassland outflow to construction land, with the largest outflow for each land category being from arable land (115,021.23 hm^2). The outflow of arable land was much smaller than the inflow, with the inflow area being only 1.40% of the outflow area, which was mainly transferred to construction land and natural wetlands. Specifically, urban and rural construction land accounted for 76.74% of the total outflow of arable land. The water area also fluctuated to a certain extent, with the main outflow transfer of water bodies going to natural wetlands. However, the inflow and outflow areas were mostly balanced, which was likely due to 86.33% of the natural wetlands flowing back into the water bodies. Over the last 35 years, a total of 4703.57 hm^2 of small and micro wetlands was outflowed, of which 61.01% was transferred to urban construction land, with only 23.15% of the construction land being transferred back to the small and micro wetlands. Cultivated land was the main inflow source for small and micro wetlands (6462.14 hm^2), which accounted for 52.13% of the inflow source.

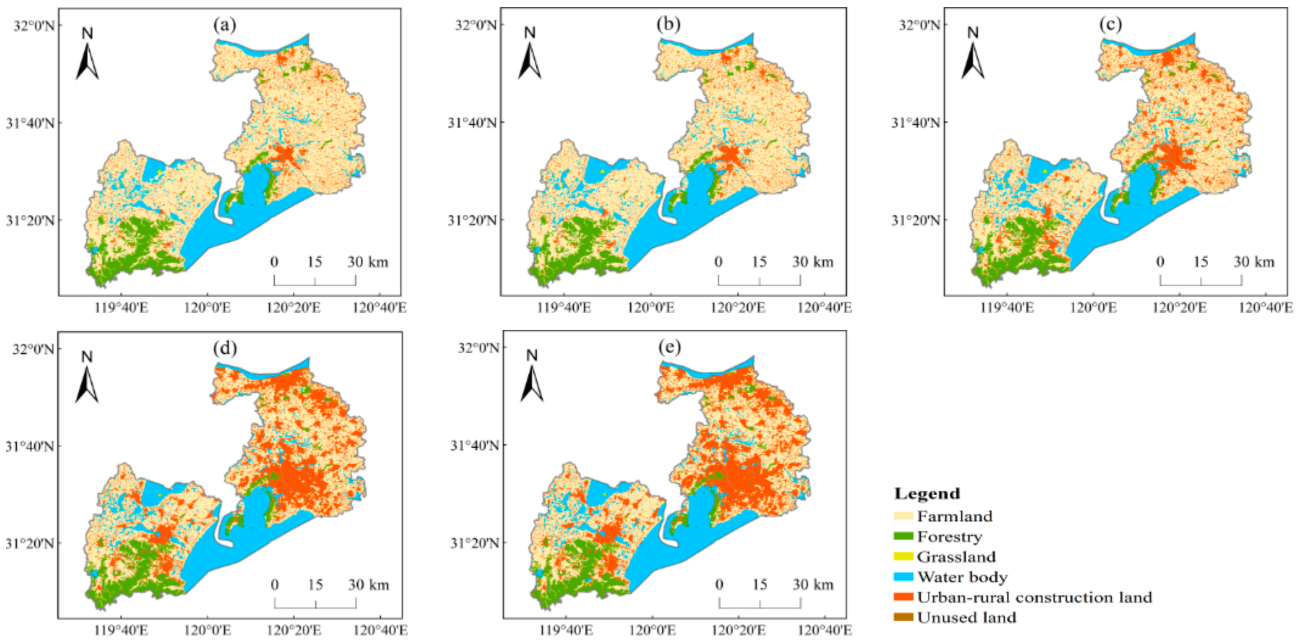

Figure 7. Changes in land use types in Wuxi area from 1980 to 2020: 1980 (**a**), 1990 (**b**), 2000 (**c**), 2010 (**d**), 2020 (**e**).

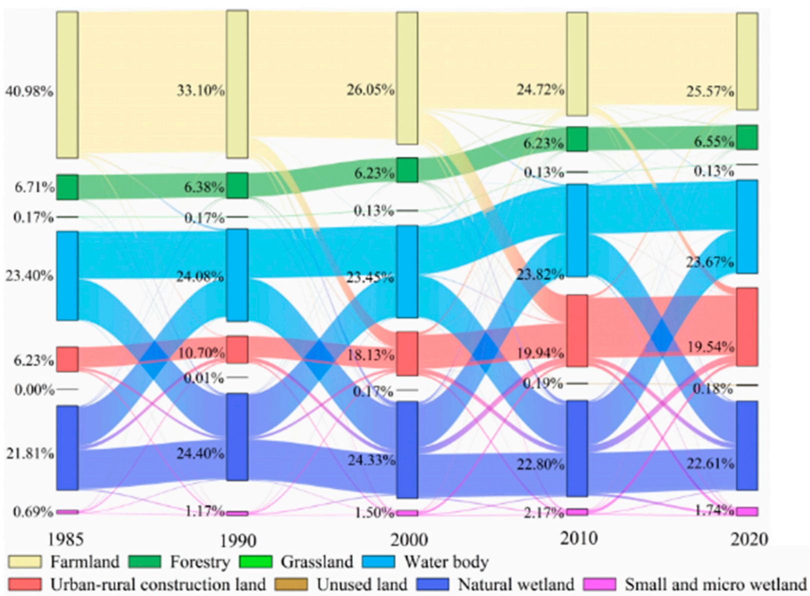

Figure 8. Sankey map of land use changes in Wuxi area from 1985 to 2020.

Understanding land use and land cover changes is useful in the development of effective environmental management strategies for coping with wetland degradation and loss [64]. Thus, a CA-Markov model was also applied in this study to predict the LULC for Wuxi area. The change trends for natural wetlands were consistent with those of water bodies; therefore, we predicted the future status of water bodies to identify the changing trends in wetlands. To verify the accuracy of our forecast, the CROSSTAB module of IDRISI 17.0 was used to verify the existing data and the LULC forecast for 2020. The verified CA-Markov model was used to predict the LULC in Wuxi in 2030, with a Kappa coefficient of 0.92, which could better reflect the LULC estimate. Figure 9 displays the simulated LULC maps and land use dynamics for 2020 and 2030, respectively, with future projections revealing that the level of urbanization increased further compared to that in 2020, with arable land and water remaining the main inflow sources. The future estimated total water outflow area was ~11,090.66 hm^2, representing a reduction of ~12% in contrast to that in 2020. In terms of allocation, 57% of the outflow area will be for cultivated land, and 35% will be for urban and rural construction land. This indicated that the wetlands will be greatly affected and further damaged by human activities in the future, primarily through the occupation of cultivated and urban construction land.

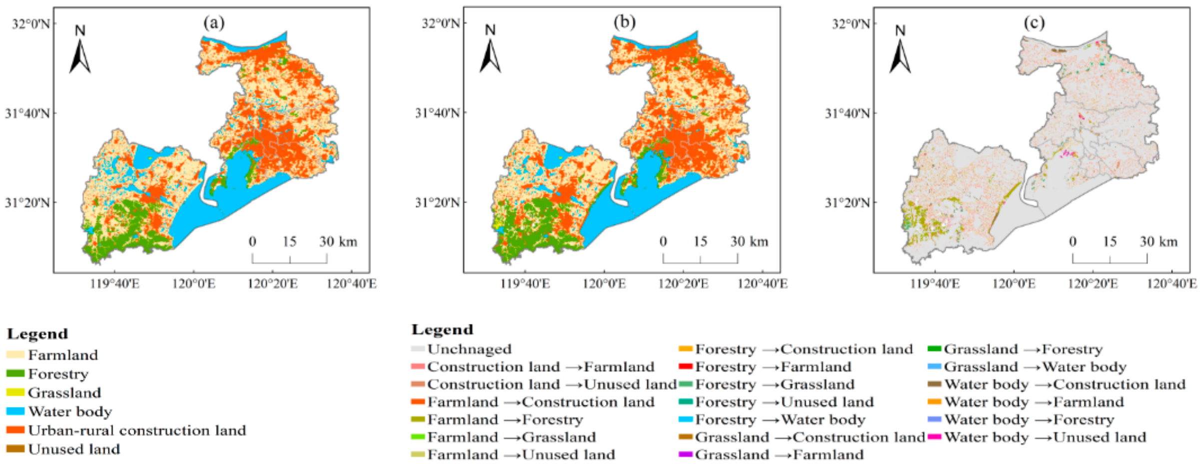

Figure 9. Forecast map of land use changes in Wuxi area: 2020 ((**a**), Simulation), 2030 (**b**), 2020–2030 (**c**).

3.3. Analysis of Driving Factors behind Natural Small and Micro Wetland Changes

The influences of the driving factors behind small and micro wetland changes were thoroughly analyzed using factor detectors, which were obtained by calculating their q values (Figure 10). In 2000, 2010, and 2020, the influences of impact factors on small and micro wetlands fluctuated to a certain extent. The exception was the land use/cover type (LULC) factor that exhibited increasing fluctuations. The other influencing factors on small and micro wetlands were as follows: distance from main roads (RD), GDP, population density (POP), annual average precipitation (PRE), annual average temperature (TEM), slope (SL), and elevation (ELE), all of which showed a decreasing trend. In 2000, the explanatory abilities of each driving factor to wetland changes from high to low were TEM > GDP > ELE > POP > SL > PRE > RD > LULC. In 2010, they were: GDP > RD > TEM > LULC > PRE > POP > SL > ELE, while, in 2020, they were: TEM > GDP> POP > LULC > PRE > RD > SL > ELE. This indicated that the natural factors contributed more to wetland changes prior to 2010, with the average annual temperature having the most significant explanatory power ($q > 0.04$). From 2010, the explanatory power of socioeconomic factors was enhanced. In 2010, the most significant explanatory power was the GDP and the distance from the main roads, both of which exceeded 5%, followed by the average annual temperature and LULC. In 2020, the most significant explanatory power was the average annual temperature, followed by the GDP and population density. The q values of slope and altitude were the lowest ($q < 0.01$) and had a negligible effect on the changes in small and micro wetlands. The average explanatory powers of each driving factor for natural small and micro wetlands were TEM > GDP > POP > RD > PRE > LULC > ELE > SL. The results of the factor detector indicated that the changes in small and micro wetlands were impacted by natural and anthropogenic activities, mainly through the average annual temperature and GDP.

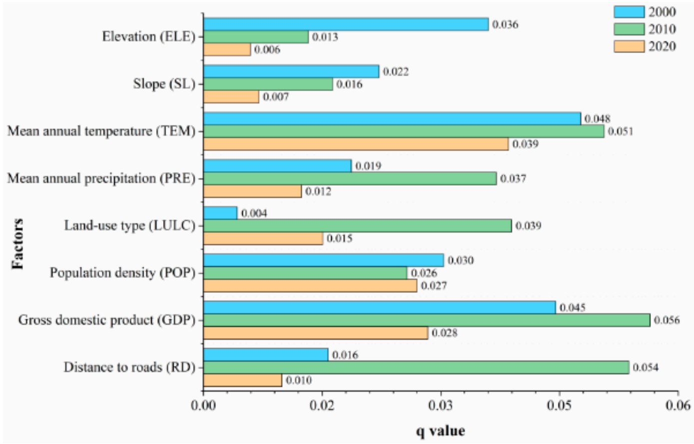

Figure 10. The q values of driving factors for the spatial differentiation of small and micro wetlands in Wuxi area from 2000 to 2020.

The results of the interaction detector showed (Figure 11) that the interactions between the driving factors were only enhanced bi-linearly and nonlinearly. This indicated that the interactions between any two factors of the eight selected for this study were greater than that of any single factor and that there was no weakening effect. These results implied that the combined effects of all factors had more explanatory power for the changes in small and micro wetlands than single factors and played a more positive driving role. In 2000, GDP and ELE and POP and ELE showed bi-linear enhancement, and the interactions between other factors showed nonlinear enhancement. The interactions between GDP and TEM were the strongest, and the interaction degree was ~14%. In 2010, GDP and POP and SL and ELE showed bi-linear enhancements, and the interactions between the other factors showed nonlinear enhancements. The interactions between RD and TEM were the strongest. In 2020, LULC and SL showed a bi-linear enhancement among all factors, while the interactions between other factors showed nonlinear enhancements, with the interactions between GDP and POP being the strongest. In summary, TEM and GDP exhibited strong combined effects with all factors and had a high explanatory power, which indicated that the changes in the small and micro wetlands of the study area were the result of the combined effects of different driving factors. The changes in any factor had an impact on small and micro wetlands, particularly the annual average temperature and GDP.

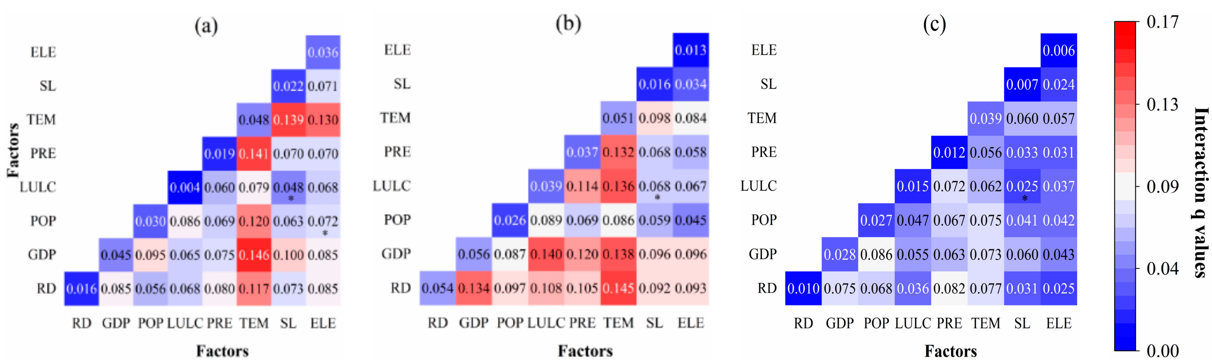

Figure 11. The q values of interactions between factors in Wuxi area from 2000 to 2020: 2000 (**a**), 2010 (**b**), 2020 (**c**). Note: * represents the interaction types of bi-linear enhancement.

4. Discussion

The accurate extraction and monitoring of changes in wetland areas and their spatial distribution are prerequisites for wetland conservation and restoration [65]. Landsat series images possess high spatial and temporal resolution and are easy to process and obtain, which makes them suitable for wetland data extraction and dynamic monitoring at small and medium regional scales [66]. For this study, based on Landsat series images, MNDWI and NDVI were employed to enhance the distinction between wetlands and vegetation [52,67], and the SVM method was used to classify and extract the status of overall, small, and micro wetlands in Wuxi area. Rahimi et al. [1] and Ahmed et al. [68] also utilized such methods to study wetlands and obtained images with a high accuracy. Therefore, the research strategy for this study had certain scientific underpinnings.

The analytical results of the extracted wetland attributes indicated that the natural wetlands in Wuxi area showed a degrading trend over the last decade, which was similar to the findings of Darrah et al. [69] and Wen et al. [70], implying that wetland coverage is currently facing the threat of degradation on a global scale. The spatial and temporal distribution of the total wetland area in China indicated that wetland areas in the middle and lower reaches of the Yangtze River provinces showed a declining trend after 2010, and this decline was closely related to local economic development and urban expansion [71]. Duan et al. [72] and Wu et al. [73] studied the southeast coastal wetlands and found that the biggest loss of coastal wetlands was due to the change in the method of utilization, which was mostly occupied for aquaculture farms and ports. We found that the scale of small and micro wetlands in Wuxi area, particularly in Yixing district and Jiangyin district, increased during the study period, while the area and number of small and micro wetlands around the Taihu Lake area did not change much. The location of small and micro wetlands in Yixing transferred from the south to the north from 1985 to 2020, with Ge Lake as the central point. This is likely to be further influenced by the growing aquaculture industry in conjunction with local development. From Figure 7, it was easy to recognize that urban construction lands along the Yangtze River in Jiangyin district have been steadily expanding since 1990. Considering that the distribution of small and micro wetlands along the Yangtze River has increased significantly since 1990, it was speculated that this trend may be closely related to increase localized industrial development and urbanization. This study found that although the total number of small and micro wetlands increased, the patches of large, small, and micro wetlands decreased in size, which meant that the wetland resources in Wuxi were fragmented and dispersed. This was consistent with the results of previous studies on wetland resources in the middle and lower reaches of the Yangtze River [37,74,75].

The results of the geographic detector analysis in this study showed that both natural and anthropogenic factors had certain influences that altered small and micro wetlands [76]. Natural factors were mainly manifested through climate change, temperature, and precipitation [77]. You et al. [78] explored the impacts of climate change on the wetlands of Poyang Lake and found that the stability of the wetlands was vulnerable to climate change, especially with higher temperatures. Vegetation grows rapidly, and the wetlands are in a healthy state; however, with higher temperatures, the precipitation decreases, and the wetland area shrinks. Mu et al. [79] also studied Poyang Lake and believed that seasonal drought and flood disasters under climate change were serious threats to wetlands. In this study, the factors of temperature, precipitation, and topography were quantified, and in the results of the factor detector, the contributions of natural factors were decreased. The q value of the mean annual temperature decreased from 0.048 to 0.039, while that of the annual average precipitation also decreased from 0.019 to 0.012. This indicated that the impacts of climate change on small and micro wetlands in Wuxi area were gradually diminished. Furthermore, according to meteorological data, it was found that the temperature in Wuxi has increased by 1.2 °C and that precipitation has increased by 49% over the last two decades, revealing a warming and wetting trend. However, the natural wetland resources of Wuxi area continued to show a decreasing trend, while the natural small and micro wetlands exhibited increasing trends. This indicated that climate change may have positive effects on small and micro wetlands but has little effect on large wetlands. The current and projected impacts of climate warming on wetlands have been extensively studied in recent years, with some researchers suggesting that climate change may amplify wetland losses [80]. Wang et al. [81] also concluded that the influence of the climate on large wetlands is diminishing.

Several researchers believe that human activities make the relationship between socioeconomic development and wetland conservation more complex than obvious climate change [36,82–84]. Some studies suggest that the land use and land cover (LULC) changes, especially the rapid expansion of urban areas, intensify the ecological vulnerability of wetlands [85–87]. For example, research by Ricaurte et al. [88] found that 24% of wetland degradation in Colombia was caused by urban land expansion. Dang et al. [89] concluded that anthropogenic activities (e.g., the intensification of agricultural activities and the expansion of aquaculture) were the primary driving factors behind wetland loss. Similarly, Yu et al. [90] analyzed the landscape pattern index of the Xixi wetland in Hangzhou and concluded that socio-economic development, accompanied by the appearance of artificial landscapes, was detrimental to the stability and protection of the ecosystem functions native to the wetland. A considerable number of studies indicate that, with the rapid urbanization process, human ecological consciousness is gradually improving, and the emergence of artificial wetlands such as wetland parks is conducive to wetland protection [91,92]. As mentioned by Vymazal et al. [93] and Gabr et al. [94], the use of constructed wetland to treat sewage can alleviate the damage to natural wetland to a certain extent. Therefore, this study also explored the relationship between human activities and small and micro wetlands. This study observed that, during the study period, the main human activities that induced changes in small and micro wetlands were GDP and population density, which emerged as the leading factors in 2010. Simultaneously, interactions between natural factors and human activities were discussed. In this study, the interactions between the two factors were mainly manifested as nonlinear enhancement, implying that the changes in small and micro wetlands were the result of the comprehensive effects of various factors. It can be seen in Figure 11 that the interactions between the GDP and all other factors were significant. In combination with the fluctuation and growth of land use contributions in the factor detector analyzed above, and in conjunction with accelerating urbanization, it was implied that, although natural and anthropogenic factors have a great influence on the distribution of small and micro wetlands, human activities and socioeconomic factors are gradually emerging as the dominant factors. This was akin to the results of earlier studies [54,81], with the difference being that the results of this study also indicated that small and micro wetlands may be more impacted by human activities in the future, and the intensification of human activities may expand the scale of small and micro wetlands. On one hand, this may be caused by the inflow generated during the transformation of land use types, while on the other hand, it may be driven by management policies, such as the return of farmland to wetlands and the construction of artificial wetlands, which increases the small areas of wetland patches.

Since this study was based on remote sensing image extraction for the analysis of wetland changes, which was limited by the quality of remote sensing images and algorithms, the results of the study will have some errors. In the future, we will use higher-resolution remote sensing images to extract wetland data. Furthermore, changes in wetlands are influenced by many factors. The influencing factors selected for this paper are not comprehensive and do not consider drought, hydrological connectivity, water pollution, food production, etc. Future studies should consider additional factors that affect the change distribution of small and micro wetlands. Despite the above limitations, this study predicted future land use changes and effectively quantified the relative contributions of each influencing factor to small and micro wetlands. This research shows that both natural and human factors have impacts on small and micro wetlands. Numerous studies have revealed that human activities have certain negative impacts on wetland resources [95–97], and our findings were similar. However, the difference is that, with urbanization, increased disturbances brought by human activities have certain positive impacts on small and micro wetlands, which increase the number of small and micro wetland patches. However, whether this growth is consistent with the concept of sustainable development requires further research and discussion. The results of this study can update our understanding of the influencing factors of small and micro wetlands and provide useful references for wetland management in the Yangtze River Delta region.

5. Conclusions

Based on the remote sensing data from 1985 to 2020 and the geographic detector model, the impacts of natural factors and human activities on small and micro wetlands in Wuxi area were quantitatively analyzed. The main conclusions were as follows:

(1) From 1985 to 2010, the area of natural wetlands in Wuxi increased by 19% (1.26×10^4 hm^2) but decreased by 10% (0.94×10^4 hm^2) after 2010. Furthermore, the proportion of small and micro wetlands in the total area of natural wetlands increased from 5% in 1985 to 12% in 2020.

(2) The natural small and micro wetlands in Wuxi area showed a trend of scale expansion from 1985 to 2020, which was manifested by the increase in the area and quantity (1.5 times and 1.7 times, respectively), with obvious seasonal characteristics. The majority of small and micro wetlands were 0.1–1 hm^2 and 1–3 hm^2, while the number of small and micro wetland patches of large-area categories decreased.

(3) Small and micro wetlands were affected by natural factors and human activities. Before 2010, natural factors were the main factors, whereas the contributions of human factors increased after 2010. The average annual temperature was the main natural factor that affected the changes in wetlands, while the GDP and population density were the most significant human factors that impacted the distribution of wetlands. Small and micro wetlands were influenced by the interactive enhancement between the two factors.

Author Contributions: Conceptualization, J.Z. and Z.Z.; methodology, B.Z.; software, J.Z.; validation, B.Z. and X.L.; formal analysis, J.Z.; resources, L.C. and Z.Z.; writing—original draft preparation, J.Z.; writing—review and editing, Z.Z. and Q.Y.; visualization, J.Z.; supervision, Z.Z.; project administration, Z.Z. All authors have read and agreed to the published version of the manuscript.

Funding: This research was funded by the National Natural Science Foundation of China (Grant no. 41971025), the Strategic Priority Research Program of the Chinese Academy of Sciences (no. XDA19030500), and the Priority Academic Program Development of Jiangsu Higher Education Institutions (PAPD).

Data Availability Statement: Not applicable.

Acknowledgments: We would like to thank the National Climate Center in Beijing for providing valuable climate datasets. In addition, we sincerely thank the editor and anonymous reviewers for their valuable comments and suggestions for improving the quality of this paper.

Conflicts of Interest: The authors declare no conflict of interest.

References

1. Rahimi, L.; Malekmohammadi, B.; Yavari, A.R. Assessing and Modeling the Impacts of Wetland Land Cover Changes on Water Provision and Habitat Quality Ecosystem Services. *Nat. Resour. Res.* **2020**, *29*, 3701–3718. [CrossRef]
2. Sun, J.; Yuan, X.; Liu, G.; Tian, K. Emergy and eco-exergy evaluation of wetland restoration based on the construction of a wetland landscape in the northwest Yunnan Plateau, China. *J. Environ. Manag.* **2019**, *252*, 109499. [CrossRef] [PubMed]
3. Tornwall, B.; Pitt, A.; Brown, B.; Hawley-Howard, J.; Baldwin, R. Diversity Patterns Associated with Varying Dispersal Capabilities as a Function of Spatial and Local Environmental Variables in Small Wetlands in Forested Ecosystems. *Forests* **2020**, *11*, 1146. [CrossRef]
4. Richardson, S.J.; Clayton, R.; Rance, B.D.; Broadbent, H.; McGlone, M.S.; Wilmshurst, J.M. Small wetlands are critical for safeguarding rare and threatened plant species. *Appl. Veg. Sci.* **2015**, *18*, 203–241. [CrossRef]

5. Kim, B.; Lee, J.; Park, J. Role of small wetlands on the regime shift of ecological network in a wetlandscape. *Environ. Res. Commun.* **2022**, *4*, 041006. [CrossRef]
6. Cheng, F.Y.; Basu, N.B. Biogeochemical hotspots: Role of small water bodies in landscape nutrient processing. *Water Resour. Res.* **2017**, *53*, 5038–5056. [CrossRef]
7. Rabbani, G.; Rahman, S.H.; Faulkner, L. Impacts of Climatic Hazards on the Small Wetland Ecosystems (ponds): Evidence from Some Selected Areas of Coastal Bangladesh. *Sustainability* **2013**, *5*, 1510–1521. [CrossRef]
8. Jeffries, M.J. Flood, drought and the inter-annual variation to the number and size of ponds and small wetlands in an English lowland landscape over three years of weather extremes. *Hydrobiologia* **2016**, *768*, 255–272. [CrossRef]
9. Cui, L.; Gao, C.; Zhao, X.; Ma, Q.; Zhang, M.; Li, W.; Song, H.; Wang, Y.; Li, S.; Zhang, Y. Dynamics of the lakes in the middle and lower reaches of the Yangtze River basin, China, since late nineteenth century. *Environ. Monit. Assess* **2013**, *185*, 4005–4018. [CrossRef]
10. Zhu, L.; Ke, Y.; Hong, J.; Zhang, Y.; Pan, Y. Assessing degradation of lake wetlands in Bashang Plateau, China based on long-term time series Landsat images using wetland degradation index. *Ecol. Indic.* **2022**, *139*, 108903. [CrossRef]
11. Gxokwe, S.; Dube, T.; Mazvimavi, D.; Grenfell, M. Using cloud computing techniques to monitor long-term variations in ecohydrological dynamics of small seasonally-flooded wetlands in semi-arid South Africa. *J. Hydrol.* **2022**, *612*, 128080. [CrossRef]
12. Janisch, J.E.; Foster, A.D.; Ehinger, W.J. Characteristics of small headwater wetlands in second-growth forests of Washington, USA. *Forest Ecol. Manag.* **2011**, *261*, 1265–1274. [CrossRef]
13. Mwita, E.; Menz, G.; Misana, S.; Becker, M.; Kisanga, D.; Boehme, B. Mapping small wetlands of Kenya and Tanzania using remote sensing techniques. *Int. J. Appl. Earth Obs.* **2013**, *21*, 173–183. [CrossRef]
14. Dale, J.; Burnside, N.G.; Strong, C.J.; Burgess, H.M. The use of small-Unmanned Aerial Systems for high resolution analysis for intertidal wetland restoration schemes. *Ecol. Eng.* **2020**, *143*, 105695. [CrossRef]
15. Mahdianpari, M.; Salehi, B.; Mohammadimanesh, F.; Motagh, M. Random forest wetland classification using ALOS-2 L-band, RADARSAT-2 C-band, and TerraSAR-X imagery. *ISPRS J. Photogramm. Remote Sens.* **2017**, *130*, 13–31. [CrossRef]
16. Wang, X.; Xiao, X.; Zou, Z.; Hou, L.; Qin, Y.; Dong, J.; Doughty, R.B.; Chen, B.; Zhang, X.; Chen, Y.; et al. Mapping coastal wetlands of China using time series Landsat images in 2018 and Google Earth Engine. *ISPRS J. Photogramm. Remote Sens.* **2020**, *163*, 312–326. [CrossRef]
17. Jie, W.-H.; Xiao, C.-L.; Zhang, C.; Zhang, E.; Li, J.-Y.; Wang, B.; Niu, H.-W.; Dong, S.-F. Remote sensing-based dynamic monitoring and environmental change of wetlands in southern Mongolian Plateau in 2000–2018. *China Geol.* **2021**, *4*, 353–363. [CrossRef]
18. Chu, L.; Sun, T.; Wang, T.; Li, Z.; Cai, C. Evolution and Prediction of Landscape Pattern and Habitat Quality Based on CA-Markov and InVEST Model in Hubei Section of Three Gorges Reservoir Area (TGRA). *Sustainability* **2018**, *10*, 3854. [CrossRef]
19. Guo, M.; Li, J.; Sheng, C.; Xu, J.; Wu, L. A Review of Wetland Remote Sensing. *Sensors* **2017**, *17*, 777. [CrossRef]
20. Zhang, X.; Wang, G.; Xue, B.; Zhang, M.; Tan, Z. Dynamic landscapes and the driving forces in the Yellow River Delta wetland region in the past four decades. *Sci. Total Environ.* **2021**, *787*, 147644. [CrossRef]
21. Li, Y. The Water Information Extraction and Land Cover Classification of Nansihu Lake Based on SPOT5 Remote Sensing Image. Master's Thesis, Shandong University, Jinan, China, 2008.
22. Song, C.; Ke, L.; Pan, H.; Zhan, S.; Liu, K.; Ma, R. Long-term surface water changes and driving cause in Xiong'an, China: From dense Landsat time series images and synthetic analysis. *Sci. Bull.* **2018**, *63*, 708–716. [CrossRef] [PubMed]
23. Ogilvie, A.; Poussin, J.-C.; Bader, J.-C.; Bayo, F.; Bodian, A.; Dacosta, H.; Dia, D.; Diop, L.; Martin, D.; Sambou, S. Combining Multi-Sensor Satellite Imagery to Improve Long-Term Monitoring of Temporary Surface Water Bodies in the Senegal River Floodplain. *Remote Sens.* **2020**, *12*, 3157. [CrossRef]
24. Cavallo, C.; Papa, M.N.; Gargiulo, M.; Palau-Salvador, G.; Vezza, P.; Ruello, G. Continuous Monitoring of the Flooding Dynamics in the Albufera Wetland (Spain) by Landsat-8 and Sentinel-2 Datasets. *Remote Sens.* **2021**, *13*, 3525. [CrossRef]
25. Fan, T.; Wang, S.; Wang, X.; Chen, X. Optimization effect of ecological restoration based on high-resolution remote sensing images in the ecological construction of soil and water conservation. *J. Amb. Intel. Hum. Comp.* **2022**, *13*, 87. [CrossRef]
26. Alibakhshi, S.; Groen, T.A.; Rautiainen, M.; Naimi, B. Remotely-Sensed Early Warning Signals of a Critical Transition in a Wetland Ecosystem. *Remote Sens.* **2017**, *9*, 352. [CrossRef]
27. Zhao, Y.; Wang, S.; Zhang, F.; Shen, Q.; Li, J.; Yang, F. Remote Sensing-Based Analysis of Spatial and Temporal Water Colour Variations in Baiyangdian Lake after the Establishment of the Xiong'an New Area. *Remote Sens.* **2021**, *13*, 1729. [CrossRef]
28. Doyle, C.; Beach, T.; Luzzadder-Beach, S. Tropical Forest and Wetland Losses and the Role of Protected Areas in Northwestern Belize, Revealed from Landsat and Machine Learning. *Remote Sens.* **2021**, *13*, 379. [CrossRef]
29. Piaser, E.; Villa, P. Evaluating capabilities of machine learning algorithms for aquatic vegetation classification in temperate wetlands using multi-temporal Sentinel-2 data. *Int. J. Appl. Earth Obs.* **2023**, *117*, 103202. [CrossRef]
30. Gao, Y.; Cui, L.; Liu, J.; Li, W.; Lei, Y. China's coastal-wetland change analysis based on high-resolution remote sensing. *Mar. Freshw. Res.* **2020**, *71*, 1161. [CrossRef]
31. Banks, S.; White, L.; Behnamian, A.; Chen, Z.; Montpetit, B.; Brisco, B.; Pasher, J.; Duffe, J. Wetland Classification with Multi-Angle/Temporal SAR Using Random Forests. *Remote Sens.* **2019**, *11*, 670. [CrossRef]
32. Wei, C.; Guo, B.; Fan, Y.; Zang, W.; Ji, J. The Change Pattern and Its Dominant Driving Factors of Wetlands in the Yellow River Delta Based on Sentinel-2 Images. *Remote Sens.* **2022**, *14*, 4388. [CrossRef]

33. Balogun, A.-L.; Yekeen, S.T.; Pradhan, B.; Althuwaynee, O.F. Spatio-Temporal Analysis of Oil Spill Impact and Recovery Pattern of Coastal Vegetation and Wetland Using Multispectral Satellite Landsat 8-OLI Imagery and Machine Learning Models. *Remote Sens.* **2020**, *12*, 1225. [CrossRef]
34. Ghosh, S.; Das, A. Wetland conversion risk assessment of East Kolkata Wetland: A Ramsar site using random forest and support vector machine model. *J. Clean. Prod.* **2020**, *275*, 123475. [CrossRef]
35. Zhang, Z.; Hu, B.; Jiang, W.; Qiu, H. Identification and scenario prediction of degree of wetland damage in Guangxi based on the CA-Markov model. *Ecol. Indic.* **2021**, *127*, 107764. [CrossRef]
36. Mao, D.; Wang, Z.; Wu, J.; Wu, B.; Zeng, Y.; Song, K.; Yi, K.; Luo, L. China's wetlands loss to urban expansion. *Land Degrad. Dev.* **2018**, *29*, 2644–2657. [CrossRef]
37. Chen, M.; Xu, X.; Wu, X.; Mi, C. Centennial-scale study on the spatial-temporal evolution of riparian wetlands in the Yangtze River of China. *Int. J. Appl. Earth Obs.* **2022**, *113*, 102874. [CrossRef]
38. Fairchild, G.W.; Robinson, C.; Brainard, A.S.; Coutu, G.W. Historical Changes in the Distribution and Abundance of Constructed Ponds in Response to Changing Population Density and Land Use. *Landsc. Res.* **2013**, *38*, 593–606. [CrossRef]
39. Johnston, C.A.; McIntyre, N.E. Effects of cropland encroachment on prairie pothole wetlands: Numbers, density, size, shape, and structural connectivity. *Landsc. Ecol.* **2019**, *34*, 827–841. [CrossRef]
40. Terasmaa, J.; Bartout, P.; Marzecova, A.; Touchart, L.; Vandel, E.; Koff, T.; Choffel, Q.; Kapanen, G.; Maleval, V.; Vainu, M.; et al. A quantitative assessment of the contribution of small standing water bodies to the European waterscapes—Case of Estonia and France. *Heliyon* **2019**, *5*, e2482. [CrossRef]
41. Liang, D.; Lu, J.; Chen, X.; Liu, C.; Lin, J. An investigation of the hydrological influence on the distribution and transition of wetland cover in a complex lake–floodplain system using time-series remote sensing and hydrodynamic simulation. *J. Hydrol.* **2020**, *587*, 125038. [CrossRef]
42. Wijewardene, L.; Wu, N.; Qu, Y.; Guo, K.; Messyasz, B.; Lorenz, S.; Riis, T.; Ulrich, U.; Fohrer, N. Influences of pesticides, nutrients, and local environmental variables on phytoplankton communities in lentic small water bodies in a German lowland agricultural area. *Sci. Total Environ.* **2021**, *780*, 146481. [CrossRef] [PubMed]
43. Hu, W.; Li, G.; Li, Z. Spatial and temporal evolution characteristics of the water conservation function and its driving factors in regional lake wetlands—Two types of homogeneous lakes as examples. *Ecol. Indic.* **2021**, *130*, 108069. [CrossRef]
44. Wang, J.; Zhang, T.; Fu, B. A measure of spatial stratified heterogeneity. *Ecol. Indic.* **2016**, *67*, 250–256. [CrossRef]
45. Huang, S.; Xiao, L.; Zhang, Y.; Wang, L.; Tang, L. Interactive effects of natural and anthropogenic factors on heterogenetic accumulations of heavy metals in surface soils through geodetector analysis. *Sci. Total Environ.* **2021**, *789*, 147937. [CrossRef] [PubMed]
46. Liu, J.; Xu, Q.; Yi, J.; Huang, X. Analysis of the heterogeneity of urban expansion landscape patterns and driving factors based on a combined Multi-Order Adjacency Index and Geodetector model. *Ecol. Indic.* **2022**, *136*, 108655. [CrossRef]
47. Wang, S.; Zhang, L.; Zhang, H.; Han, X.; Zhang, L. Spatial—Temporal Wetland Landcover Changes of Poyang Lake Derived from Landsat and HJ-1A/B Data in the Dry Season from 1973–2019. *Remote Sens.* **2020**, *12*, 1595. [CrossRef]
48. Wang, Y.; Zhang, Z.; Chen, X. Quantifying Influences of Natural and Anthropogenic Factors on Vegetation Changes Based on Geodetector: A Case Study in the Poyang Lake Basin, China. *Remote Sens.* **2021**, *13*, 5081. [CrossRef]
49. Wang, Y.; Wen, H.; Sun, D.; Li, Y. Quantitative Assessment of Landslide Risk Based on Susceptibility Mapping Using Random Forest and GeoDetector. *Remote Sens.* **2021**, *13*, 2625. [CrossRef]
50. Long, X.; Lin, H.; An, X.; Chen, S.; Qi, S.; Zhang, M. Evaluation and analysis of ecosystem service value based on land use/cover change in Dongting Lake wetland. *Ecol. Indic.* **2022**, *136*, 108619. [CrossRef]
51. Liu, Y.; Yang, P.; Zhang, S.; Wang, W. Dynamic identification and health assessment of wetlands in the middle reaches of the Yangtze River basin under changing environment. *J. Clean. Prod.* **2022**, *345*, 131105. [CrossRef]
52. Xing, L.; Niu, Z.; Jiao, C.; Zhang, J.; Han, S.; Cheng, G.; Wu, J. A Novel Workflow for Seasonal Wetland Identification Using Bi-Weekly Multiple Remote Sensing Data. *Remote Sens.* **2022**, *14*, 1037. [CrossRef]
53. Xiaoli, H.; Xin, L.; Ling, L. Modeling the Land Use Change in an Arid Oasis Constrained by Water Resources and Environmental Policy Change Using Cellular Automata Models. *Sustainability* **2018**, *10*, 2878. [CrossRef]
54. Koko, A.; Yue, W.; Abubakar, G.; Hamed, R.; Noman, A.A. Monitoring and Predicting Spatio-Temporal Land Use/Land Cover Changes in Zaria City, Nigeria, through an Integrated Cellular Automata and Markov Chain Model (CA-Markov). *Sustainability* **2020**, *12*, 10452. [CrossRef]
55. Siddique, M.A.; Wang, Y.; Xu, N.; Ullah, N.; Zeng, P. The Spatiotemporal Implications of Urbanization for Urban Heat Islands in Beijing: A Predictive Approach Based on CA—Markov Modeling (2004–2050). *Remote Sens.* **2021**, *13*, 4697. [CrossRef]
56. Ju, H.; Zhang, Z.; Zuo, L.; Wang, J.; Zhang, S.; Wang, X.; Zhao, X. Driving forces and their interactions of built-up land expansion based on the geographical detector—A case study of Beijing, China. *Int. J. Geogr. Inf. Sci. IJGIS* **2016**, *30*, 2188–2207. [CrossRef]
57. Huan, W.; Jiangbo, G.; Wenjuan, H. Quantitative attribution analysis of soil erosion in different geomorphological types in karst areas: Based on the geodetector method. *J. Geogr. Sci.* **2019**, *29*, 271–286. [CrossRef]
58. Song, Y.; Wang, J.; Ge, Y.; Xu, C. An optimal parameters-based geographical detector model enhances geographic characteristics of explanatory variables for spatial heterogeneity analysis: Cases with different types of spatial data. *Gisci. Remote Sens.* **2020**, *57*, 593–610. [CrossRef]

59. Ren, D.; Cao, A. Analysis of the heterogeneity of landscape risk evolution and driving factors based on a combined GeoDa and Geodetector model. *Ecol. Indic.* **2022**, *144*, 109568. [CrossRef]
60. Ji, B.; Qin, Y.; Zhang, T.; Zhou, X.; Yi, G.; Zhang, M.; Li, M. Analyzing Driving Factors of Drought in Growing Season in the Inner Mongolia Based on Geodetector and GWR Models. *Remote Sens.* **2022**, *14*, 6007. [CrossRef]
61. Zhu, L.; Meng, J.; Zhu, L. Applying Geodetector to disentangle the contributions of natural and anthropogenic factors to NDVI variations in the middle reaches of the Heihe River Basin. *Ecol. Indic.* **2020**, *117*, 106545. [CrossRef]
62. Wang, K.; Cao, C.; Xie, B.; Xu, M.; Yang, X.; Guo, H.; Duerler, R.S. Analysis of the Spatial and Temporal Evolution Patterns of Grassland Health and Its Driving Factors in Xilingol. *Remote Sens.* **2022**, *14*, 5179. [CrossRef]
63. Wang, D.; Dong, Z.; Ling, Z.; Jiang, F.; Zhu, S.; Chen, J. Spatiotemporal variability of extreme precipitation at different time scales and quantitative analysis of associated driving teleconnection factors: Insights from Taihu Basin, China. *Ecol. Indic.* **2022**, *142*, 109287. [CrossRef]
64. Gxokwe, S.; Dube, T.; Mazvimavi, D. Multispectral Remote Sensing of Wetlands in Semi-Arid and Arid Areas: A Review on Applications, Challenges and Possible Future Research Directions. *Remote Sens.* **2020**, *12*, 4190. [CrossRef]
65. Chen, K.; Cong, P.; Qu, L.; Liang, S.; Sun, Z. Annual variation of the landscape pattern in the Liao River Delta wetland from 1976 to 2020. *Ocean. Coast. Manag.* **2022**, *224*, 106175. [CrossRef]
66. Mahdianpari, M.; Jafarzadeh, H.; Granger, J.E.; Mohammadimanesh, F.; Brisco, B.; Salehi, B.; Homayouni, S.; Weng, Q. A large-scale change monitoring of wetlands using time series Landsat imagery on Google Earth Engine: A case study in Newfoundland. *Gisci. Remote Sens.* **2020**, *57*, 1102–1124. [CrossRef]
67. Han, X.; Feng, L.; Hu, C.; Chen, X. Wetland changes of China's largest freshwater lake and their linkage with the Three Gorges Dam. *Remote Sens. Environ.* **2018**, *204*, 799–811. [CrossRef]
68. Ahmed, K.R.; Akter, S.; Marandi, A.; Schüth, C. A simple and robust wetland classification approach by using optical indices, unsupervised and supervised machine learning algorithms. *Remote Sens. Appl. Soc. Environ.* **2021**, *23*, 100569. [CrossRef]
69. Darrah, S.E.; Shennan-Farpón, Y.; Loh, J.; Davidson, N.C.; Finlayson, C.M.; Gardner, R.C.; Walpole, M.J. Improvements to the Wetland Extent Trends (WET) index as a tool for monitoring natural and human-made wetlands. *Ecol. Indic.* **2019**, *99*, 294–298. [CrossRef]
70. Wen, L.; Hughes, M.G. Coastal Wetland Responses to Sea Level Rise: The Losers and Winners Based on Hydro-Geomorphological Settings. *Remote Sens.* **2022**, *14*, 1888. [CrossRef]
71. An, X.; Jin, W.; Zhang, H.; Liu, Y.; Zhang, M. Analysis of long-term wetland variations in China using land use/land cover dataset derived from Landsat images. *Ecol. Indic.* **2022**, *145*, 109689. [CrossRef]
72. Duan, Y.; Tian, B.; Li, X.; Liu, D.; Sengupta, D.; Wang, Y.; Peng, Y. Tracking changes in aquaculture ponds on the China coast using 30 years of Landsat images. *Int. J. Appl. Earth Obs.* **2021**, *102*, 102383. [CrossRef]
73. Wu, W.; Zhi, C.; Gao, Y.; Chen, C.; Chen, Z.; Su, H.; Lu, W.; Tian, B. Increasing fragmentation and squeezing of coastal wetlands: Status, drivers, and sustainable protection from the perspective of remote sensing. *Sci. Total Environ.* **2022**, *811*, 152339. [CrossRef] [PubMed]
74. Zhang, L.; Wu, B.; Yin, K.; Li, X.; Kia, K.; Zhu, L. Impacts of human activities on the evolution of estuarine wetland in the Yangtze Delta from 2000 to 2010. *Environ. Earth Sci.* **2015**, *73*, 435–447. [CrossRef]
75. Yang, H.; Wang, H.; Lu, J.; Zhou, Z.; Feng, Q.; Wu, Y. Full Lifecycle Monitoring on Drought-Converted Catastrophic Flood Using Sentinel-1 SAR: A Case Study of Poyang Lake Region during Summer 2020. *Remote Sens.* **2021**, *13*, 3485. [CrossRef]
76. Chen, H.; Zhang, W.; Gao, H.; Nie, N. Climate Change and Anthropogenic Impacts on Wetland and Agriculture in the Songnen and Sanjiang Plain, Northeast China. *Remote Sens.* **2018**, *10*, 356. [CrossRef]
77. Junk, W.J.; An, S.; Finlayson, C.M.; Gopal, B.; Květ, J.; Mitchell, S.A.; Mitsch, W.J.; Robarts, R.D. Current state of knowledge regarding the world's wetlands and their future under global climate change: A synthesis. *Aquat. Sci.* **2013**, *75*, 151–167. [CrossRef]
78. You, H.; Fan, H.; Xu, L.; Wu, Y.; Liu, L.; Yao, Z. Poyang Lake Wetland Ecosystem Health Assessment of Using the Wetland Landscape Classification Characteristics. *Water* **2019**, *11*, 825. [CrossRef]
79. Mu, S.; Li, B.; Yao, J.; Yang, G.; Wan, R.; Xu, X. Monitoring the spatio-temporal dynamics of the wetland vegetation in Poyang Lake by Landsat and MODIS observations. *Sci. Total Environ.* **2020**, *725*, 138096. [CrossRef]
80. Edvardsson, J.; Šimanauskienė, R.; Taminskas, J.; Baužienė, I.; Stoffel, M. Increased tree establishment in Lithuanian peat bogs—Insights from field and remotely sensed approaches. *Sci. Total Environ.* **2015**, *505*, 113–120. [CrossRef]
81. Wang, C.; Ma, L.; Zhang, Y.; Chen, N.; Wang, W. Spatiotemporal dynamics of wetlands and their driving factors based on PLS-SEM: A case study in Wuhan. *Sci. Total Environ.* **2021**, *806*, 151310. [CrossRef]
82. William, J.M.; Maria, E.H. Landscape and climate change threats to wetlands of North and Central America. *Aquat. Sci.* **2013**, *75*, 133–149. [CrossRef]
83. Li, Q.; Long, Z.; Wang, H.; Zhang, G. Functions of constructed wetland animals in water environment protection—A critical review. *Sci. Total Environ.* **2021**, *760*, 144038. [CrossRef] [PubMed]
84. Zhu, L.; Zhang, H.; Li, Y.; Cheng, G.; Zhu, Y.; Song, C.; Wang, L.; Du, G. Long-term variation characteristics of nutrients in the water and sediments of a surface flow constructed wetland with micro-polluted water sources. *Ecol. Eng.* **2023**, *187*, 106848. [CrossRef]

85. Ghosh, S.; Das, A. Urban expansion induced vulnerability assessment of East Kolkata Wetland using Fuzzy MCDM method. *Remote Sens. Appl. Soc. Environ.* **2019**, *13*, 191–203. [CrossRef]
86. Ding, Q.; Chen, Y.; Bu, L.; Ye, Y. Multi-Scenario Analysis of Habitat Quality in the Yellow River Delta by Coupling FLUS with InVEST Model. *Int. J. Environ. Res. Public Health* **2021**, *18*, 2389. [CrossRef]
87. Yang, L.; Zhang, S.; Yin, L.; Zhang, B. Global occupation of wetland by artificial impervious surface area expansion and its impact on ecosystem service value for 2001–2018. *Ecol. Indic.* **2022**, *142*, 109307. [CrossRef]
88. Ricaurte, L.F.; Olaya-Rodríguez, M.H.; Cepeda-Valencia, J.; Lara, D.; Arroyave-Suárez, J.; Finlayson, C.M.; Palomo, I. Future impacts of drivers of change on wetland ecosystem services in Colombia. *Glob. Environ. Chang.* **2017**, *44*, 158–169. [CrossRef]
89. Dang, A.T.N.; Kumar, L.; Reid, M.; Nguyen, H. Remote Sensing Approach for Monitoring Coastal Wetland in the Mekong Delta, Vietnam: Change Trends and Their Driving Forces. *Remote Sens.* **2021**, *13*, 3359. [CrossRef]
90. Yu, M.-J.; Wu, J.-J.; Xu, J.M.; Shi, J.C. Studies on the Changes of Landscape Patterns of Hangzhou Xixi Wetland in 15 years. *Bull. Sci. Technol.* **2007**, *23*, 320–325. [CrossRef]
91. Ranjan, R. Restoring natural wetlands through financial incentives based adoption of constructed wetlands on agricultural farms. *J. Clean. Prod.* **2021**, *317*, 128346. [CrossRef]
92. Xu, Y.; Zhang, X.; Liu, X.; Zhang, Z. Biodiversity and Spatiotemporal Distribution of Spontaneous Vegetation in Tangdao Bay National Wetland Park, Qingdao City, China. *Int. J. Environ. Res. Public Health* **2022**, *19*, 11665. [CrossRef] [PubMed]
93. Vymazal, J. Constructed Wetlands for Wastewater Treatment: Five Decades of Experience. *Environ. Sci. Technol.* **2011**, *45*, 61–69. [CrossRef] [PubMed]
94. Gabr, M.E.; Al-Ansari, N.; Salem, A.; Awad, A. Proposing a Wetland-Based Economic Approach for Wastewater Treatment in Arid Regions as an Alternative Irrigation Water Source. *Hydrology* **2023**, *10*, 20. [CrossRef]
95. Zhang, G.; Yao, T.; Chen, W.; Zheng, G.; Shum, C.K.; Yang, K.; Piao, S.; Sheng, Y.; Yi, S.; Li, J.; et al. Regional differences of lake evolution across China during 1960s–2015 and its natural and anthropogenic causes. *Remote Sens. Environ.* **2019**, *221*, 386–404. [CrossRef]
96. Dong, L.; Wan, R.; Li, B.; Tan, Z.; Yang, S.; Zhang, T. Spatiotemporal dynamics of lake wetland in the Wanjiang Plain of the Yangtze River basin, China during the recent century. *Ecol. Indic.* **2022**, *142*, 109295. [CrossRef]
97. Yang, S.; Wan, R.; Yang, G.; Li, B.; Dong, L. Combining historical maps and landsat images to delineate the centennial-scale changes of lake wetlands in Taihu Lake Basin, China. *J. Environ. Manag.* **2023**, *329*, 117110. [CrossRef]